



Experimental Study on Relationship of Applied Power And Feeding Rate on Production of Polyurethane Nanofibre

M.Ö. ÖTEYAKA^{1,*}, E. ÖZEL², M. M. YILDIRIM¹

¹ *Dumlupınar University, Faculty of Engineering, Department of Mechanical Engineering, Tavşanlı Yolu,
Merkez Kampüs, Kütahya, TURKEY*

² *Dumlupınar University, Faculty of Engineering, Department of Industrial Engineering, Tavşanlı Yolu,
Merkez Kampüs, Kütahya, TURKEY*

Received: 13.07.2011 Revised: 23.02.2012 Accepted: 18.03.2013

ABSTRACT

In this work, a polymer of polyurethane (PU) was electrospun for 1 hour to create a scaffold under different conditions. A 3x3 general full factorial in a completely randomised design using three levels of two factors: power (W= 20, 22 and 25 Watts) and feeding rate (V=1.00, 1.25 and 1.50 ml/h) was used to assess the response pattern and to determine the combined effect of independent variables. The main effects for power (W) and feeding rate (V) and the power (W)*feeding rate (V) interaction were statistically significant.

Key words: Electrospinning, Polyurethane, Nanofibre, Statistical Analysis.

1. INTRODUCTION

The polymer polyurethane is an thermoplastic polymer with good mechanical properties such as tensile strength, high load-bearing capabilities, abrasion resistance and, good compression compared to other materials widely used in industry for a wide range of textile, packaging and biomaterials applications [1-3].

Dropping to nanoscale diameters of polymer fibre materials, several excellent characteristics appear when compared to micrometre fibres, such as a very large surface area to volume ratio (this ratio for a nanofibre can be as large as 103 times of that of a microfibre), flexibility in surface functionalities, and superior mechanical performance (e.g. stiffness and tensile strength) compared with any other known form of the

*Corresponding author, e-mail: mozgur.oteyaka@dpu.edu.tr

material. These properties make polymer nanofibres optimal candidates for many important applications. A number of processing techniques such as drawing, template synthesis, phase separation, self-assembly, and electrospinning have been used to prepare polymer nanofibres in recent years [4-6].

The electrospinning technique has been used in many applications such as biosensors, cosmetics, filters, etc. [7-11]. In biomaterials research, the nano sizes of fibres are particularly interesting because communication between cells also occurs on the nano scale. Also, nano-sized fibres can mimic the extracellular matrix (ECM) which plays a critical role in cell proliferation, cell motility, and intercellular signalling, as shown in vascular graft replacement [12-15].

The electrospinning method is one method for producing randomly-oriented nanofibres with a high surface area to volume [16, 17]. Pedicini and Farris (2003) produced PU nanofibres from electrospinning method with diameters ranging from 100 to 500 nm [18]. This technique is extensively described in the literature [6, 19-21]. Most polymers are dissolved in a solvent before electrospinning, and the processing conditions involved are simple and straightforward. Basically, it involves high voltage applied between the polymeric solution and the collector to produce micrometre-to-nanometre fibres. As the intensity of the electric field is increased, the hemispherical surface of the solution at the tip of the capillary syringe elongates to form a conical shape known as the Taylor cone. Further increasing the electric field, a critical value is attained at which the repulsive electrostatic force overcomes the surface tension and the charged jet of the fluid is ejected from the tip before reaching the collecting screen, the solution jet evaporates or solidifies, and is collected as an interconnected web of small fibres.

The morphology of fibres depends on the electrospinning parameters used. For example, the influence of applied voltage, feeding rate, concentration, etc. has been evaluated [22-24]. Many parameters can influence the transformation of polymer solutions into nanofibres through electrospinning. These parameters include (a) solution properties such as viscosity, elasticity, conductivity, and surface tension, (b) governing variables such as hydrostatic pressure in the capillary tube, electric potential at the capillary tip, and the gap (distance between the tip and the collecting screen), and (c) ambient parameters such as solution temperature, humidity, and air velocity in the electrospinning chamber [25-27].

In general, a higher polymer concentration and higher applied voltage (more fluid is ejected in the jet) result in a larger fibre diameter. In fact, Deitzel et al. (2001) have pointed out that fibre diameter increased with increasing polymer concentration according to a power law relationship [28]. Demir et al. (2002) further found that the fibre diameter was proportional to the cube of the polymer concentration [26]. In addition, Cao et al. (2010) showed that increasing concentration results a larger fibre diameter. However, the applied voltages took an opposite trend compared with the concentration [29].

There is a little confusion over the behaviour of applied voltage. Reneker and Chun (1996) have demonstrated that there is not much effect of electric field on the fibre diameter [21]. On the other hand, Zhuo et al. (2005) spun a 5.0 wt. % PU/DMF solution at various applied voltages [24]. They found that uniform nanofibres without beads could not be obtained until the applied voltage reached 12.0 kV. Other authors have reported that at higher voltage, bead formation occurs [12,26,28]. Yordem et al. (2008) concluded that the influence of voltage depends on the concentration of the polymer solution and the distance between the tip and the collector [30].

The feeding rate of the polymer solution from the syringe is an important process parameter. A few studies have investigated the relationship between feeding rate and fibre diameter and morphology [23,24]. Zhuo et al. (2005) observed the influence of feeding rate on nanofibre morphology for a 5.0 wt. % PU/DMF solution. At a higher feeding rate, they found a larger fibre, while at a lower feeding rate they observed smaller and more uniform fibres [24]. Nevertheless, it was found that high flow rates resulted in beaded fibres due to insufficient drying time prior to reaching the collector [23].

As observed above, there has been confusion on the effect of these two factors (power and feed rate) alone or together on the diameter and beading of polyurethane nanofibres in a 15% wt. PU solution. Aside from the many questions which remain to be addressed on electrospinning factors, these two factors of the electrospinning method should be examined. It is necessary to statistically assess the effect of power, feeding rate and both on the diameter and beading of polyurethane nanofibre. This study, therefore, sought to respond to these challenges. According to best of our knowledge, there is no report detailing a statistical analysis of PU nanofibres.

For this purpose in this study, the electrospinning technique was used to produce polyurethane (PU) nanofibres (scaffold) using a full factorial design experiment. Different experiment parameters were conducted to evaluate the effects on diameter and morphology. The parameters selected for this work were applied voltage (W) and feeding rate (V). In this manner, this method can be used to produce a convenient fibre diameter with or without beads.

2. MATERIALS AND METHODS

The solution was composed of 15 wt. % polyurethane (PU) and 85 wt. % N-dimethylformamide (DMF) purchased from Inovenso (Innovative engineering solution). A schematic diagram to interpret the electrospinning of polymer nanofibres is shown in Fig. 1. A syringe with a 5 ml feed was filled with polymeric solution (PU/DMF) set on a micro pump ready to spin. Next, high voltage was applied between the tip and collector (aluminium foil) to electrospin the polymeric solution. The experimental conditions defined for high voltage were 20, 22 and 25 kV and were 1.00, 1.25 and 1.50 ml/h for the feeding rates. Each experiment had a total duration of 1 hour under the same conditions.

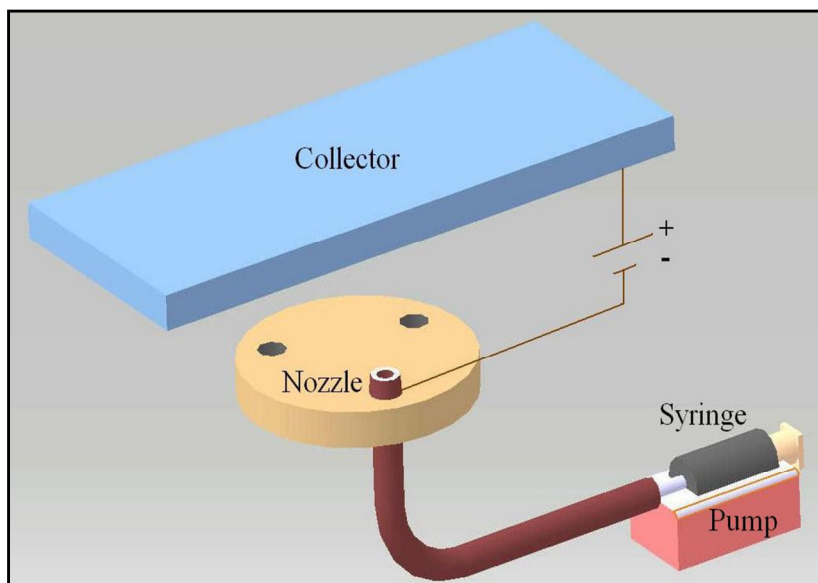


Figure 1. Electrospinning setup.

Scanning electron microscopy (SEM; model JEOL 5600 LV) was used to analyse the morphology of the samples. For this purpose, nanofibres spun onto aluminium foil were coated with gold before SEM analysis. The images were processed with ImageJ software. The diameter of fibres (R) and beads (B) on the scaffold were accurately measured with ImageJ software (free edition). A diamond TG/DTA thermal analyser was used to simultaneously record TG, DTG and DTA curves in the static air atmosphere at a heating rate of 5°C/min in the temperature range of 35–500°C using platinum crucibles.

A 3x3 general full factorial in a completely randomised design using three levels of two factors: power (W= 20, 22 and 25 kV) and feeding rate (V=1.00, 1.25 and 1.50 ml/h) was used to evaluate beading and fibre diameter and to determine the combined effect of the independent variables. Three replicates were performed to allow the experimenter obtain an estimate of experimental error and a more precise estimate of the factors [31]. The collected data were analysed by using analysis of variance (ANOVA). The basic assumptions of normality, independent variance and variance homogeneity were tested by the normal probability plot of residuals and the plot of residuals versus time, respectively. Normality was tested by the normal probability plot of residuals,

$$e = Y - \hat{Y} \quad (\text{eq.1})$$

where (e) is the difference between the observed value (Y) and the estimated value (\hat{Y}) given by the model [32]. Additionally, the main effects and interaction effects plots were drawn. All the analysis was performed on Minitab 14 statistical software.

3. RESULTS AND DISCUSSION

Figure 2 shows the SEM images of the resultant scaffold spun from 15 wt. % PU/DMF solution at various applied voltages (20kV, 22kV and 25kV) and feeding rates (1.00 ml/h, 1.25 ml/h and 1.50 ml/h). As observed in Figure 2, after electrospinning, the fibres were randomly oriented with bead formation at some places. In all conditions, the formation of beads is observed with nanofibers. However, SEM observations show that power and feeding rate affect the surface. It can be stated that a low applied voltage exhibits uniform surface. The analysis of average diameters of the nanofibres is performed for 20 kV, 22 kV and 25 kV with constant feeding rate 1.50 ml/h and the diameter are respectively 0.09 μm , 0.08 μm and 0.07 μm . As discussed above, some authors have shown that increasing the applied voltage increases diameter fibres [11] while this, conversely, can also narrow fibre diameter [14-16]. Compared to studies, our results show that increasing applied voltage decrease the diameter of nanofibers.

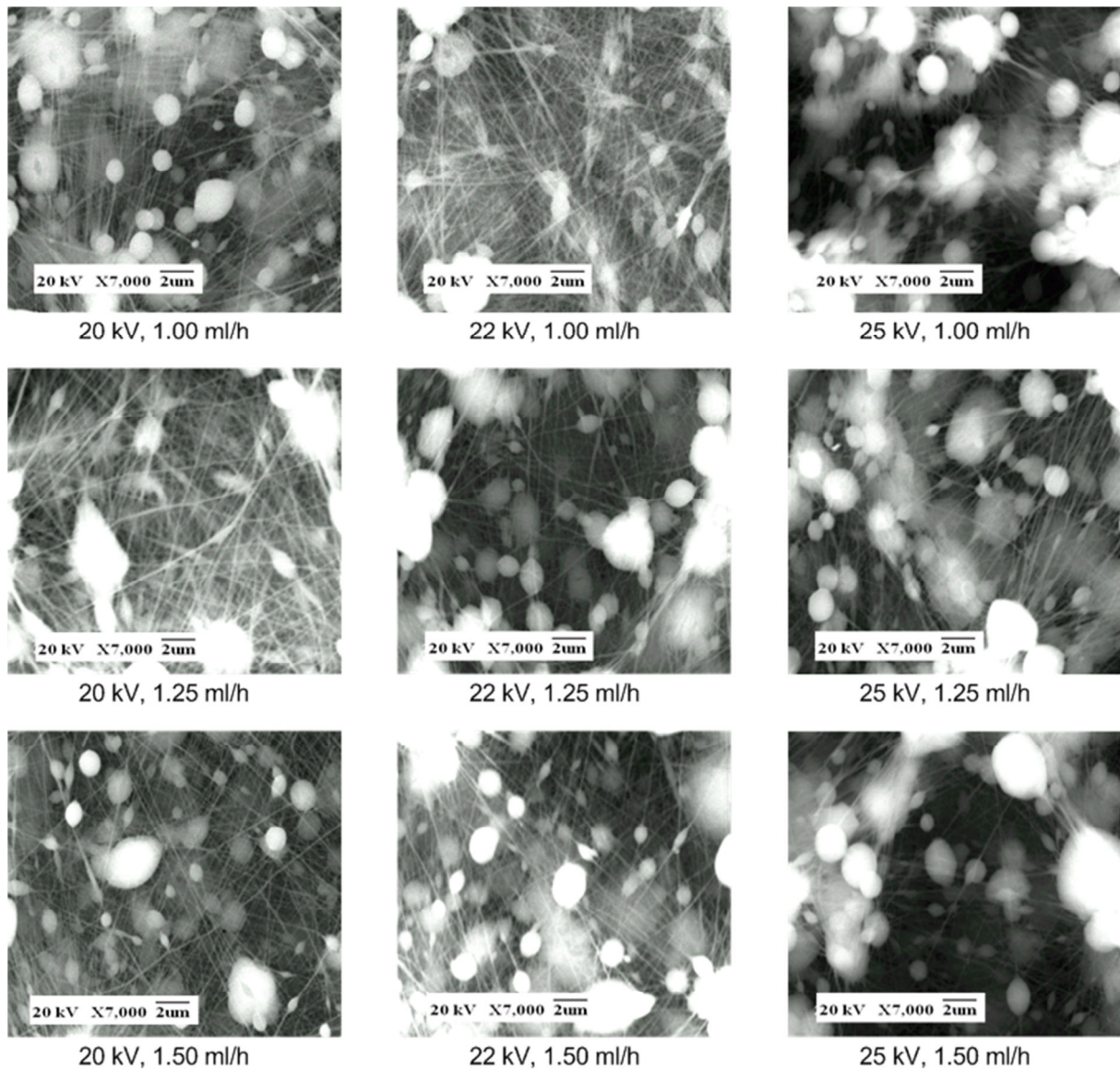


Figure 2. SEM images of PU scaffold at different applied voltages (20 kV, 22 kV and 25 kV) and feeding rates (1.00 ml/h, 1.25 ml/h and 1.50 ml/h).

The images presented in Figure 2 were processed with ImageJ software to obtain a histogram of the black-white intensity of each figure. The results show that in Figure 3, 22 kV treatments offered an equal intensity distribution of white and black compared to the other two conditions. Additionally, the treatment at 25 kV

showed higher black intensity than treatment of 20 kV. From these results, we can assume that the treatment at 25 kV resulted in finer fibres with higher porosity because of the higher black intensity. In addition, a low applied voltage resulted in more uniform nanofibres as observed in Figure 3a.

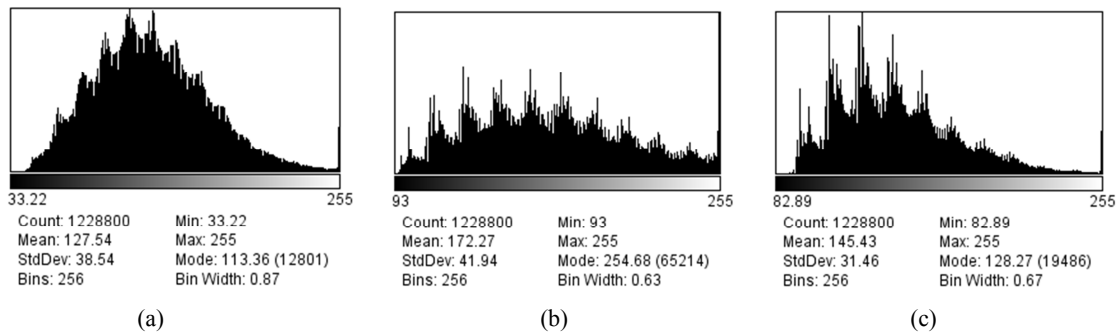


Figure 3. Black and white intensity distribution of 20 kV, 22 kV and 25 kV with constant feeding rate 1.50 ml/h..

The analysis of variance is summarised in Table 1. The last column of the table indicates the percentage of each factor contribution on the total variation, thus exhibiting the degree of influence on the result. We see that W, V and the W*V interaction significantly affected B and R ($p=0.000<0.005$). The most significant factor on the parameter B was power, which explained a 41.94% contribution to the total variation. Velocity followed this at 29.86%. About 99.61% of the variability of B was explained by this model. Only a very small part of the variability (0.39%) could be attributed to experimental error. For the R parameter, velocity was the most contributory factor on changing R explaining 82.66% of the variability. The P*W interaction follow this at 11.67%. About 99.83% of the variability of R was explained by this model.

Normal probability plots of the residuals versus normal % probability for two parameters (beads and fibre diameter) are plotted in Figure 4. The residuals show an approximately straight line, indicating that the residuals are normally distributed. The plots of residuals versus observation order are shown in Figure 5. It is shown that there is no reason to suspect any violation of the independence or constant variance assumptions. The residuals did not exhibit clear pattern. Based on these assumptions, the ANOVA model fits the data reasonably well.

Table 1. Analysis of variance results for parameters: (a) B, (b) R.

Source	DF	Seq SS	Adj SS	Adj MS	F	P	% Contribution
a) Analysis of Variance for B							
Power (W)	2	0.62287	0.62287	0.31143	955.53	0.000	41.94
Velocity (V)	2	0.44347	0.44347	0.22173	680.32	0.000	29.86
Power (W)*Velocity (V)	4	0.41307	0.41307	0.10327	316.84	0.000	27.81
Error	18	0.00587	0.00587	0.00033			0.39
Total	26	1.48527					
S = 0.0180534 R-Sq = 99.61% R-Sq(adj) = 99.43%							
b) Analysis of Variance for R							
Power (W)	2	0.00059	0.00059	0.00029	294.67	0.000	5.50
Velocity (V)	2	0.00885	0.008847	0.00442	4427.96	0.000	82.66
Power (W)*Velocity (V)	4	0.00125	0.001249	0.00031	312.55	0.000	11.67
Error	18	0.00002	0.00002	0.00001			
Total	26	0.01070					
S = 0.000999444 R-Sq = 99.83% R-Sq(adj) = 99.76%							

The main effects plots of B and R are illustrated in Figure 6. The main effects plots indicate that for power, when it changed from 20 to 25, the mean R decreased although mean of B increased. For velocity, when it changed from 1.00 to 1.50, the mean R increased although mean of B increased up to 1.25 V and mean B

decreased when it rose to 1.50. Notice on the plots below that while the main effect of velocity was greater than power for the R parameter, the main effect of power was greater than velocity for the B parameter. The analysis of variance results verified those conclusions.

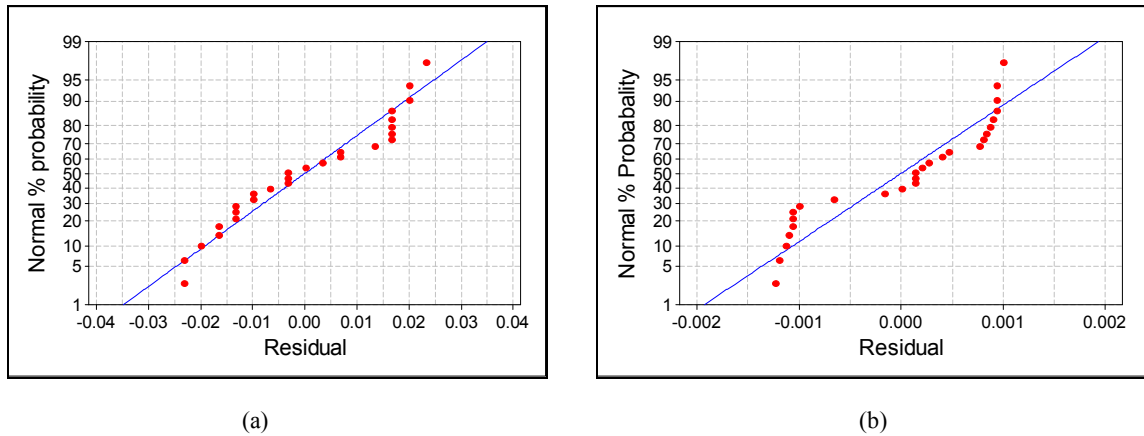


Figure 4. Normal probability plot of residual for a) B and b) R.

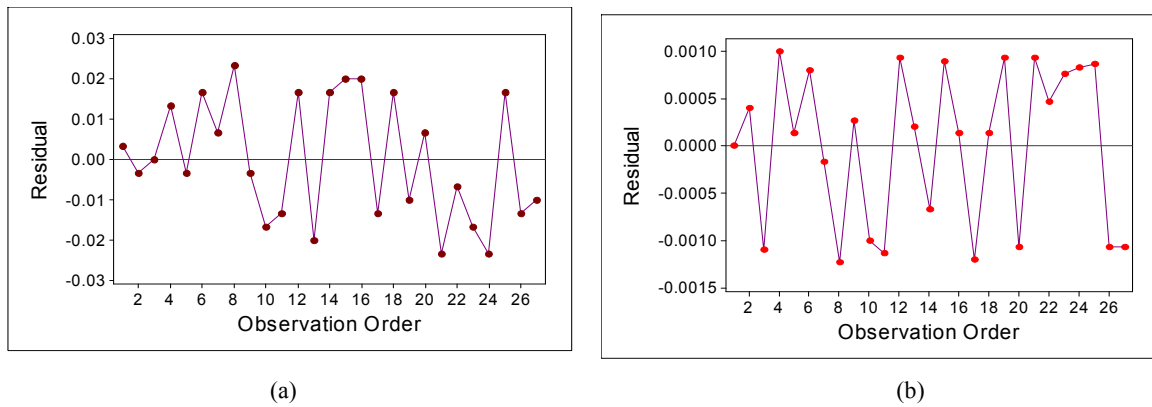


Figure 5. Plot of residuals versus observation order for a) B and b) R.

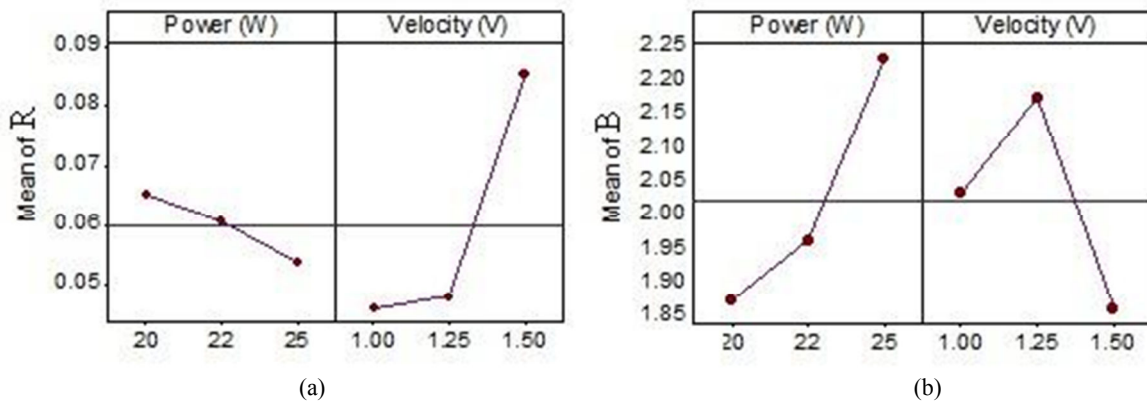


Figure 6. Main effects plots for a) B, b) R.

As observed on ANOVA table, the interactions are significant both for B and R; for this reason, it was necessary to examine the interaction plots. Because an interaction can magnify or diminish main effects, evaluating interactions is extremely important. The interaction plots are given in Figure 7. The plots show that while power at 20 W with velocity at 1.00 V gave the lowest R value (about 0.04), power at 22 W and

velocity at 1.5 V gave the largest R value (about 0.10). Power at 20 W with velocity at 1.5 V gave the lowest B value (about 1.55), and power at 25 W with velocity at 1.5 V gave the largest R value (about 2.35).

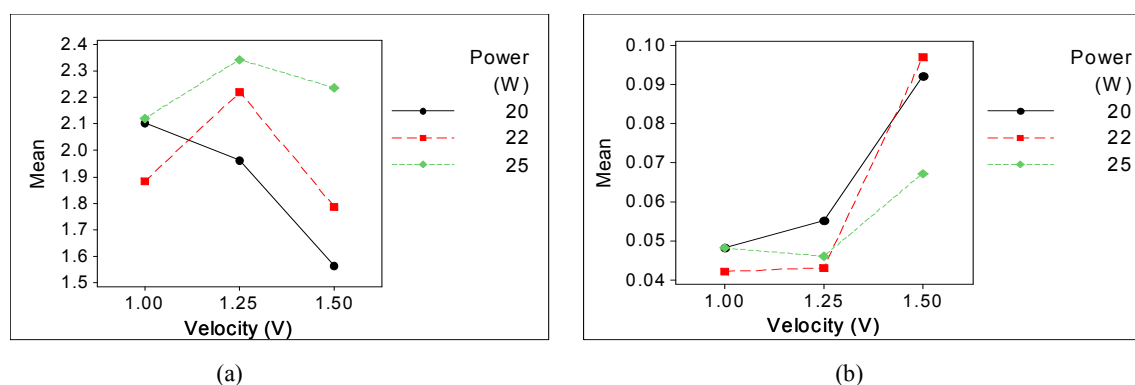


Figure 7. Interaction effects plots for a) B and b) R.

4. CONCLUSIONS

In this study, PU nanofibre scaffolds are successfully prepared from a 15 wt. % PU/DMF solution under different applied voltages and feeding rates. The applied voltage and feeding rate greatly influenced the morphology and fibre diameter. The statistical analysis confirmed the image analysis by the ImageJ software. The following conclusions could be drawn:

- Of all combinations, the best nanofibres with the fewest beads and finest fibres could be electrospun with a 20-22 kV applied voltage and 1.00-1.50 ml/hr feeding rate. A lower applied voltage resulted in more uniform nanofibres, and the largest diameter fibres.
- Based on the statistical results of the experiments, it was found that the effects of Power (P), Velocity (V) and the interaction (P*V) between them was statistically significant on both B and R. We recommend, to obtain a finer fibre diameter (R), 22 W for power and 1.00 ml/h for velocity, and to reduce bead formation (B) 20 W for power and 1.50 ml/h for velocity should be selected, under these conditions.

REFERENCES

- [1] Yoo, H.S., Kim, T.G., Park, T.G., "Surface-functionalized electrospun nanofibers for tissue engineering and drug delivery", *Adv Drug Deliv Rev*, 61: 1033–1042, (2009).
- [2] Schreuder-Gibson, H.L., Gibson, P., Seneca, K., Sennett, M., Walker, J., Yeomans, W., et al., "Protective textile materials based on electrospun nanofibers", *J Adv Mat*, 34(3): 44–55, (2002).
- [3] Wang, X.Y., Lee, S.H., Drew, C., Senecal, K.J., Kumar, J., Samuelson, L.A., "Highly sensitive optical sensors using electrospun polymeric nanofibrous membranes", *Mat Res Soc Symp Pro*, 708:397–402, (2002).
- [4] Ondarcuhu, T. and Joachim, C., "Drawing a single nanofibre over hundreds of microns", *Europhys Lett*, 42(2): 215–220, (1998).
- [5] Ma, P.X. and Zhang, R., "Synthetic nano-scale fibrous extracellular matrix", *J Biomed Mat Res*, 46 : 60–72, (1999).
- [6] Deitzel, J.M., Kleinmeyer, J., Hirvonen, J.K., Beck, T.N.C., "Controlled deposition of electrospun poly(ethylene oxide) fibers", *Polymer*, 42: 8163–8170, (2001a).
- [7] Bhardwaj, N. and Kundu, S.C., "Electrospinning: A fascinating fiber fabrication technique", *Biotechnology Advances*, 28: 325–347, (2010).
- [8] Ramanathan, K., Bangar, M.A., Yun, M., Chen, W., Myung, N.V., Mulchandani, A., "Bioaffinity sensing using biologically functionalized conducting-polymer nanowire" *J Am Chem Soc*, 127: 496–507, (2005).
- [9] Ramakrishna, S., Fujihara, K., Teo, W.E., Yong, T., Ma, Z., Ramaseshan, R., "Electrospun nanofibers: solving global issues", *Mater Today*, 9: 40–50, (2006).
- [10] Figeys, D. and Pinto, D., "Lab-on-a-chip: a revolution in biological and medical sciences—a look at some of the basic concepts and novel components used to construct prototype devices", *Anal Chem.*, 72: 330A–335A, (2000).
- [11] Friess, W., "Collagen biomaterial for drug delivery", *Eur J Pharm Biopharm*, 45: 113–136, (1998).
- [12] Li, W.J., Laurencin CT, Cateson EJ, Tuan RS, Ko FK., "Electrospun nanofibrous structure: a novel scaffold for tissue engineering", *J Biomed Mater Res*, 60: 613–621, (2002).
- [13] He, W., Horn, S.W., Hussain, M.D., "Improved bioavailability of orally administered mifepristone from PLGA nanoparticles", *Int J Pharm*, 334: 173–178, (2007).
- [14] Liang, D., Hsiao, B.S., Chu, B., "Functional electrospun nanofibrous scaffolds for biomedical applications", *Adv Drug Deliv Rev*, 59: 1392–1412, (2007).

- [15] Ding Cao, Yi-Pan Wu, Zhi-Feng Fu, Yuan Tian, Cong-Ju Li, Chun-Ying Gao, Zhong-Liang Chen, Xi-Zeng Feng, "Cell adhesive and growth behavior on electrospun nanofibrous scaffolds by designed multifunctional composites", *Colloids and Surfaces B: Biointerfaces*, 84: 26–34, (2011).
- [16] Adomaviciute, E. and Rimvydas, M., "The influence of applied voltage on poly (vinyl alcohol) (PVA) nanofibre diameter", *Fibers and Text. East Eur.*, 15: 64-75, (2007).
- [17] Cao, D., Fu, Z, Li, C., "Heat and compression molded electrospun poly(l-lactide) membranes: Preparation and characterization", *Materials Science and Engineering B*, 176: 900– 905, (2011).
- [18] Angelo Pedicini and Richard J. Farris, Mechanical behavior of electrospun polyurethane, *Polymer*, 44: 6857–6862, (2003).
- [19] Fong, H. and Reneker, D.H., "Electrospinning and formation of nanofibers", In: Salem D.R. (Ed.), *Structure formation in polymeric fibers*, Munich: Hanser, 225–246, (2001).
- [20] Kidoaki, S., Kwon I.K., Matsuda, T., "Mesoscopic spatial designs of nano and microfiber meshes for tissue-engineering matrix and scaffold based on newly devised multilayering and mixing electrospinning techniques", *Biomaterials*, 26: 37–46, (2005).
- [21] Reneker, D.H. and Chun, L., "Nanometre diameters of polymer, produced by electrospinning", *Nanotechnology*, 7: 216–223, (1996).
- [22] Zhang, C., Yuan, X., Wu, L., Han, Y., Sheng, J., "Study on morphology of electrospun poly (vinyl alcohol) mats", *Eur. Polym. J.*, 41: 423–432, 2005b.
- [23] Yuan, X.Y., Zhang, Y.Y., Dong, C.H., Sheng, J., "Morphology of ultrafine polysulfone fibers prepared by electrospinning", *Polym. Int.*, 53: 1704–1710, (2004).
- [24] Zuo, W.W., Zhu, M.F., Yang, W., Yu, H., Chen, Y.M., Zhang, Y., "Experimental study on relationship between jet instability and formation of beaded fibers during electrospinning", *Polym Eng Sci*, 45: 704–709, (2005).
- [25] Doshi, J., and Reneker, D.H., "Electrospinning process and applications of electrospun fibers", *J. Electrostatics*, 35 (2-3): 151– 160, (1995).
- [26] Demir, M.M., Yilgor, I., Yilgor, E., Erman, B., "Electrospinning of polyurethane fibers", *Polymer*, 43: 3303–3309, (2002).
- [27] Liu, H.Q., Hsieh, Y.L., "Ultrafine fibrous cellulose membranes from electrospinning of cellulose acetate" *J. Polymer Sci B: Polymer Physics*, 40: 2119–2129, (2002).
- [28] Deitzel, J.M., Kleinmeyer, J., Harris, D., Tan, N.C.B., "The effect of processing variables on the morphology of electrospun nanofibers and textiles", *Polymer*, 42: 261–272, (2001b).
- [29] Cao, D., Fu, Z, Li, C., "Electrospun Fiber Membranes of Novel Thermoplastic Polyester Elastomers: Preparation and Characterization", *Journal of Applied Polymer Science*, 122: 1698–1706, (2011).
- [30] Yordem, O.S., Papila, M., Menciloğlu, Y.Z., "Effects of electrospinning parameters on polyacrylonitrile nanofiber diameter: an investigation by response surface methodology", *Mater Des*, 29: 34–44, (2008).
- [31] McCarville, D.R. and Custer, L., "Design and Analysis of Experiments", *Wiley 7th Edition*, 45 (2008).
- [32] Czitrom, V. and Spagon, P.D., "Statistical Case Studies Analysis for Industrial Process Improvement", *Society for Industrial Mathematics*, 193, (1997).